PART TWO

DETECTION RANGE AND ARRIVAL TIME ESTIMATES

PART TWO

DETECTION RANGE AND ARRIVAL TIME ESTIMATES

TABLE OF CONTENTS

PART TWO

DETECTION RANGE AND ARRIVAL TIME ESTIMATES

LIST OF TABLES

PART TWO

DETECTION RANGE AND ARRIVAL TIME ESTIMATES

LIST OF FIGURES

PART TWO

DETECTION RANGE AND ARRIVAL TIME ESTIMATES

LIST OF FIGURES
(Continued)

PART TWO

DETECTION RANGE AND ARRIVAL TIME ESTIMATES

Roy Greenfield
Pennsylvania State University

I. SUMMARY

Estimates are given for the distance from a seismometer at which a miner can probably be detected. The procedure in making these estimates was to first establish the natural noise levels at the output of a surface seismometer for the 25 to 100 Hz frequency passband. The noise levels give the range of values which may be expected in areas with no man-made noise. For each noise level, we give the detection threshold which, when exceeded, indicates that a signal has been received. Based on the signals recorded by Westinghouse, curves are given which show the peak signal amplitude as a function of source-to-receiver distance (slant range). Curves are given for the Westinghouse seismic thumper, a 50-pound timber, and a sledge. For a given type of source, the receive signal strength depends more strongly on slant range than on any other factor. However, there is approximately a five-to-one scatter in the amplitudes. Thus, further study of factors affecting the signal amplitude might allow better estimates to be made for any particular geological setting.

Combining the signal amplitude with the detection thresholds for the different noise conditions gives the distances at which a miner should be detected. These are given in Table 1* below.

Table 1

Maximum Range (in Feet) at Which a Miner Could be Detected

For a Single Sensor--Before Signal-to-Noise Improvement Techniques

(Natural Noise and Average Signal Strength Assumed)

	Natural Noise Condition		
Source Type	Low	High	Very High
Thumper	1600	1000	700
Timber	1400	800	500
Sledge	1200	700	400

The text also gives the increase in detection ranges which should occur if steps are taken to increase S/N by 10 dB. We feel that 10 dB is a conservative estimate of the improvement possible.

During an actual rescue operation, the seismic crew and system should be capable of making on-site estimates of their detection capability, based on measurements of the site noise, and upon the best available estimates of the

* References to Figures, Tables, and Equations apply to those in this Part unless otherwise noted.

signal strengths to be expected. This will allow the seismic rescue crew to estimate the likely coverage area of the seismic system, for detection of a signalling miner under the prevailing noise conditions, which will in turn assist the rescue team to determine appropriate search strategies for the entrapped miners.

The effects of noise on the estimates of signal arrival times are also discussed. The arrival times should be picked by an analyst from stacked signals from all available signal repetitions. It is shown that for low to moderate noise situations, the signal arrival time at each subarray can be determined to within a few milliseconds. However, when the noise is comparable to the signal, errors of 10 to 15 milliseconds can occur, and in some cases, it might be possible to pick a signal arrival time which is 50 to 100 milliseconds after the true arrival time.

II. INTRODUCTION

In this Part estimates, based on experimental data, are made of the natural noise levels encountered for surface seismometers, and a model for signal levels, based on Westinghouse data,* is developed as a function of slant range and source type. The natural noise level estimates are applicable to the range of conditions encountered when no man-made noise sources are present. These natural noise levels may be representative of the levels experienced during a mine emergency rescue operation at those times when care has been taken to control the rescue activity's seismic disturbances. Further experimental data is needed in order to characterize the man-made noise environment created by rescue operations.

Using the above results, estimates have been made for the detection range which can be obtained. All work is done for a 25 to 100 Hz bandpass. Most of the signals observed by Westinghouse have most of their energy in that band. It remains (as noted in Part Nine) to determine the noise levels above 100 Hz before it is possible to determine if the band above 100 Hz will aid in detection. Initially detection ranges are determined for a single sensor with no signal processing. Some estimates also are made of detection ranges if signal enhancement is successful. After the detection discussion, a chapter will consider how noise levels affect estimates of signal arrival times for use in the subsequent location process.

III. NOISE LEVELS

We desire to determine a detection threshold, which when exceeded indicates that a signal is present at the output from a single sensor. In the Appendix to this Part, we show a reasonable detection threshold level as 3 times the noise RMS level. This will lead to approximately 1 false alarm each 100 seconds on a single trace, and very rare false alarms if coincidence detection is used on the outputs of several subarrays.

To estimate, within the time available, the surface noise levels to be expected, we concentrated on the noise data of Frantti[1] 1963 rather than the noise measurements made by Westinghouse. This was done because the contamination of the Westinghouse earth noise data by system noise weakened our confidence in their noise data (see Parts Nine, Ten). The Frantti data are for locations free of obvious man-made noise sources. Frantti measured peak-to-peak average envelope values at the output of a 1/3 octave filter. In cases where this envelope average was compared to the RMS noise level, the

* Westinghouse Contract H0210063 with Bureau of Mines.

envelope average was slighly higher. In (A 6) of the Addendum we show this is to be expected, but the difference, a factor of 1.7, is not important because RMS noise levels can be expected to fluctuate over more than an order of magnitude at different times and locations.

We used 47 of Frantti's noise curves (data for deep mines and a site near the ocean were excluded). For each curve the spectral level was read at 25, 50, and 100 Hz. Histograms (Figures 1, 2, and 3) were formed for each frequency. The RMS noise levels exceeded 75% of the time (low noise) were determined for each frequency, and marked on the histograms. This was also done for the RMS noise levels exceeded only 25% of the time (high noise). As a comparison, the range of levels found by Westinghouse during their mine field test program are also included on these Figures. The Westinghouse levels are not inconsistent with the levels predicted by Frantti.

To proceed from the RMS noise spectral estimates to the noise RMS output level of a 25 to 100 Hz filter, we used

$$RMS_{75\%} = \left[\int_{25}^{100} A^2 (f)\, df\right]^{1/2} \qquad (1)$$

for the "low noise" level condition. The RMS (amplitude) spectrum, A(f), used is plotted on Figure 4. The signal detection threshold was then set at 3 times the noise RMS output level. The same calculations were made for the (25%) "high noise" level condition. The results are given in Table 2.

Table 2

RMS Noise Output and Detection Threshold

Of a 25 To 100 Hz Filter

	(μIPS)
RMS Level Exceeded 75% of Time (Low Noise)	0.22
RMS Level Exceeded 25% of Time (High Noise)	1.5
Detection Threshold (Low Noise)	0.66
Detection Threshold (High Noise)	4.5

IV. SIGNAL LEVELS

The basis of our estimates of the seismic signal levels is the Westinghouse data. The maximum zero-to-peak amplitude levels for the signals are plotted as a function of slant range in Figure 5. The sources of data are given in the Figure. Curves have been drawn as estimates of the strong

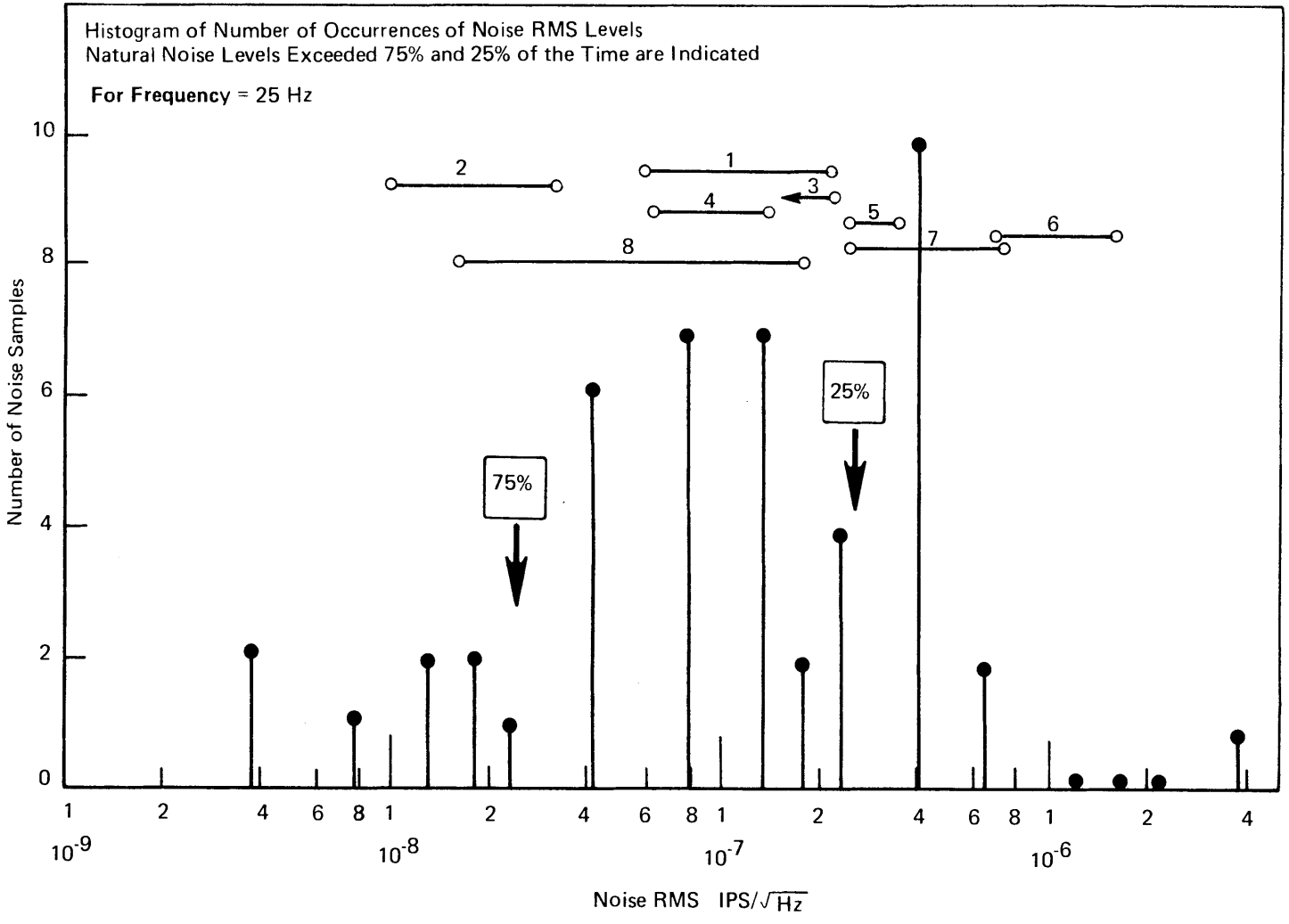

Westinghouse data for individual mines are included for comparison, and maximum and minimum noise levels are shown as open circles connected by lines. Ignore the vertical axis in relation to these data. Arrows pointing to the left indicate that system noise limited noise estimates for low noise periods. The Westinghouse data are taken from the Westinghouse Report Table 2-4. The order of the mines, going from the top of the figure to the bottom data points, corresponds to the field report numbers for the mines.

FIGURE 1 NATURAL SEISMIC NOISE LEVELS: BASED ON FRANTTI DATA WHEN NO MAN-MADE NOISE IS PRESENT

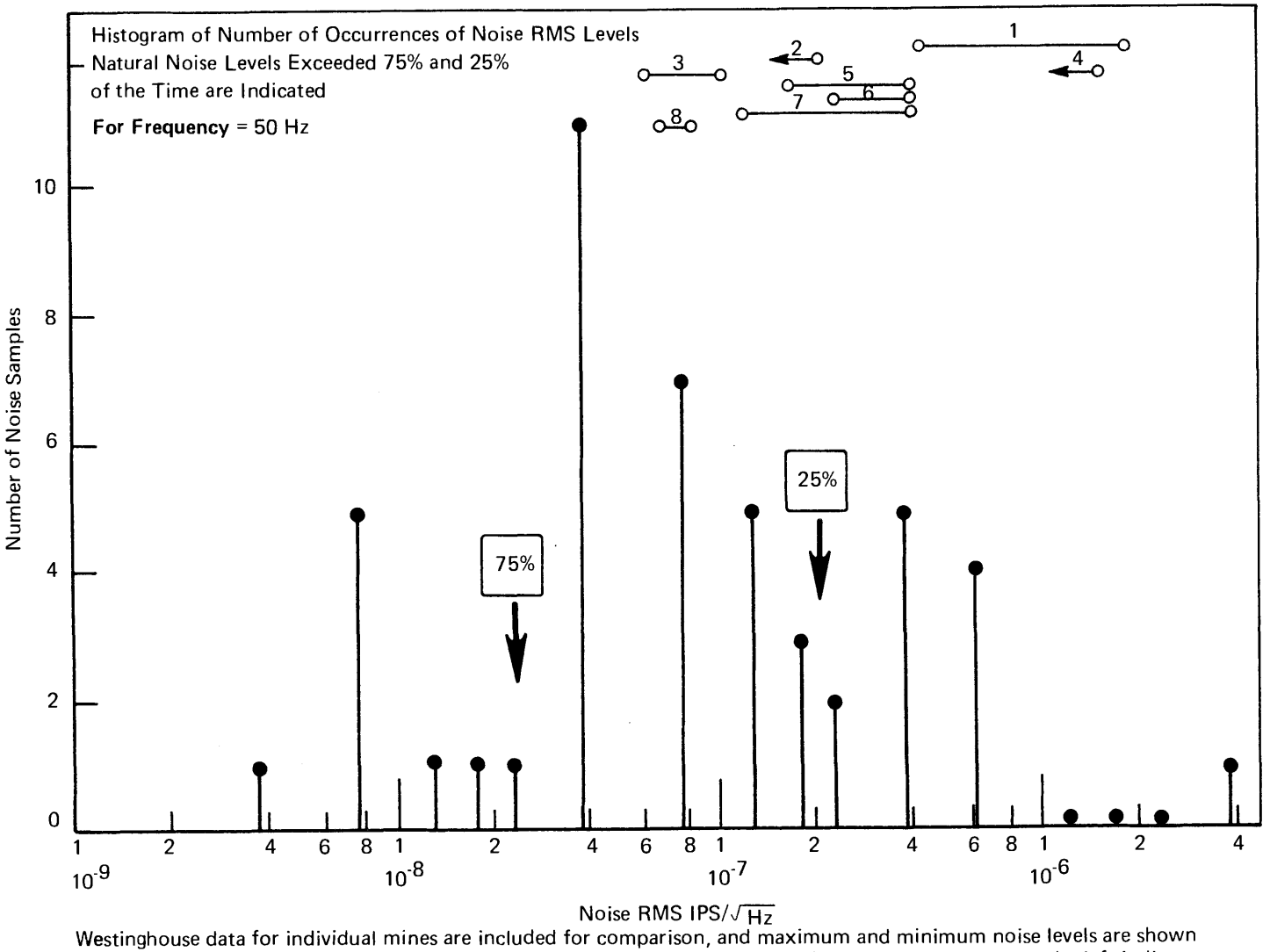

Westinghouse data for individual mines are included for comparison, and maximum and minimum noise levels are shown as open circles connected by lines. Ignore the vertical axis in relation to these data. Arrows pointing to the left indicate that system noise limited noise estimates for low noise periods. The Westinghouse data are taken from the Westinghouse Report Table 2-4. The order of the mines, going from the top of the figure to the bottom data points, corresponds to the field report numbers for the mines.

FIGURE 2 NATURAL SEISMIC NOISE LEVELS: BASED ON FRANTTI DATA WHEN NO MAN-MADE NOISE IS PRESENT

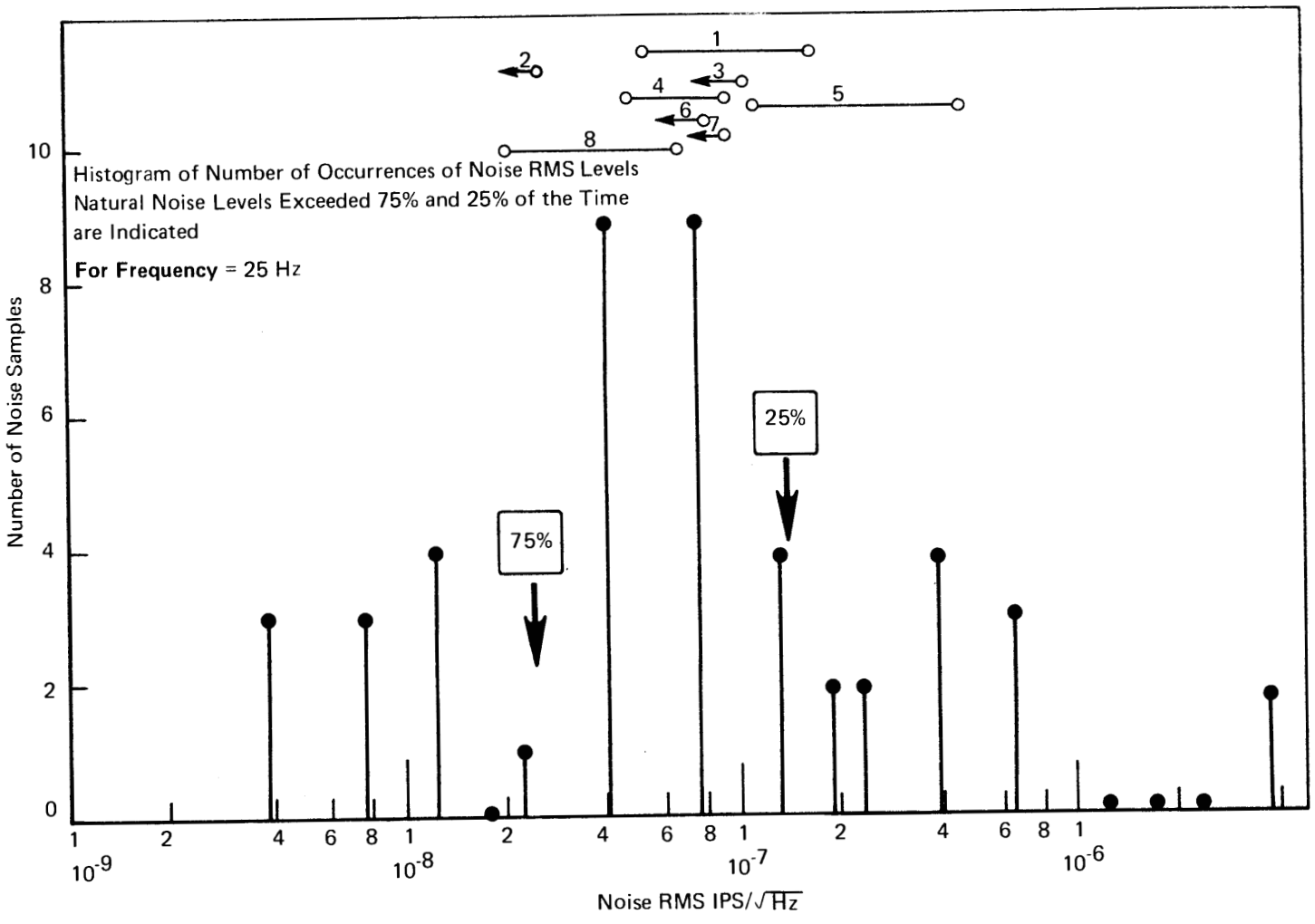

Westinghouse data for individual mines are included for comparison, and maximum and minimum noise levels are shown as open circles connected by lines. Ignore the vertical axis in relation to these data. Arrows pointing to the left indicate that system noise limited noise estimates for low noise periods. The Westinghouse data are taken from the Westinghouse Report Table 2-4. The order of the mines, going from the top of the figure to the bottom data points, corresponds to the field numbers for the mines.

FIGURE 3 NATURAL SEISMIC NOISE LEVELS: BASED ON FRANTTI DATA WHEN NO MAN-MADE NOISE IS PRESENT

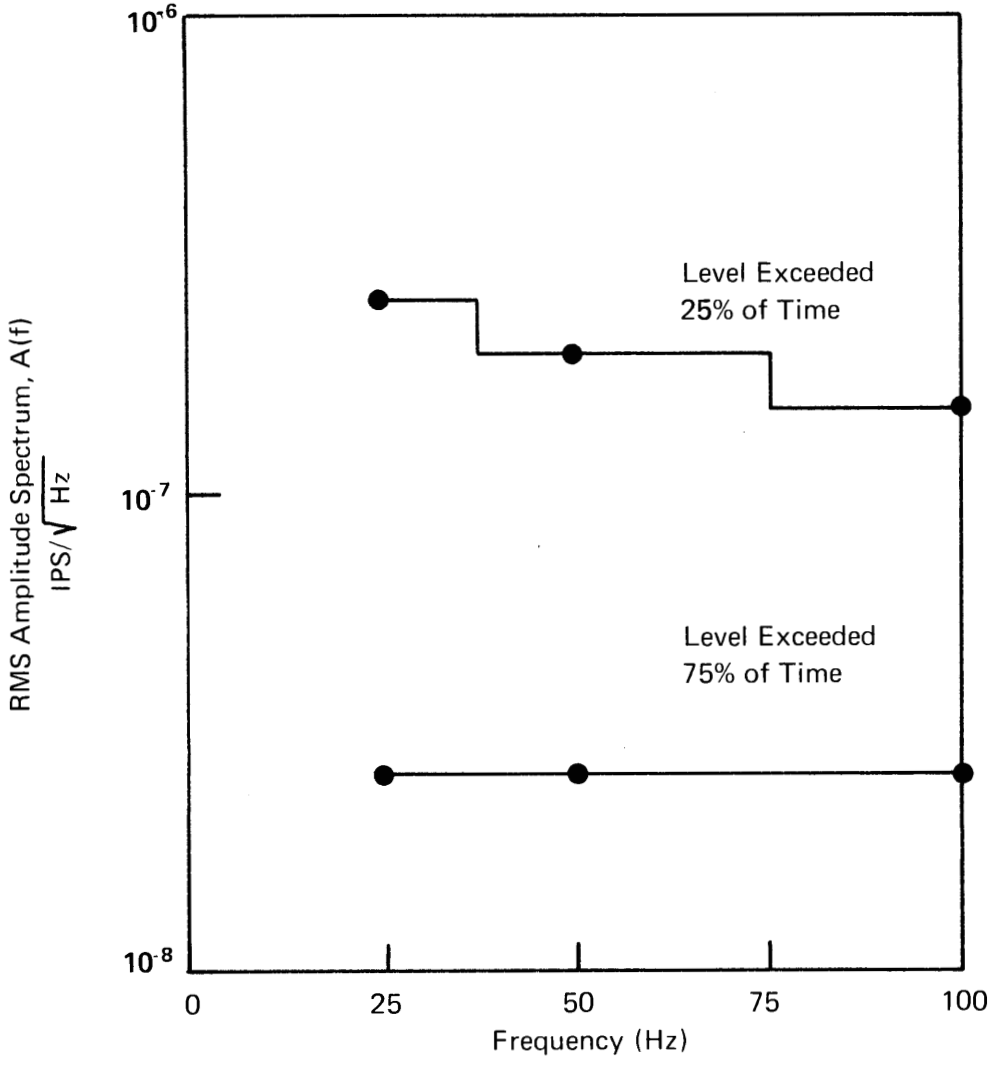

FIGURE 4 NATURAL SEISMIC NOISE LEVELS BASED ON FRANTTI DATA WHEN NO OBVIOUS MAN-MADE NOISE IS PRESENT (RMS AMPLITUDE SPECTRA)

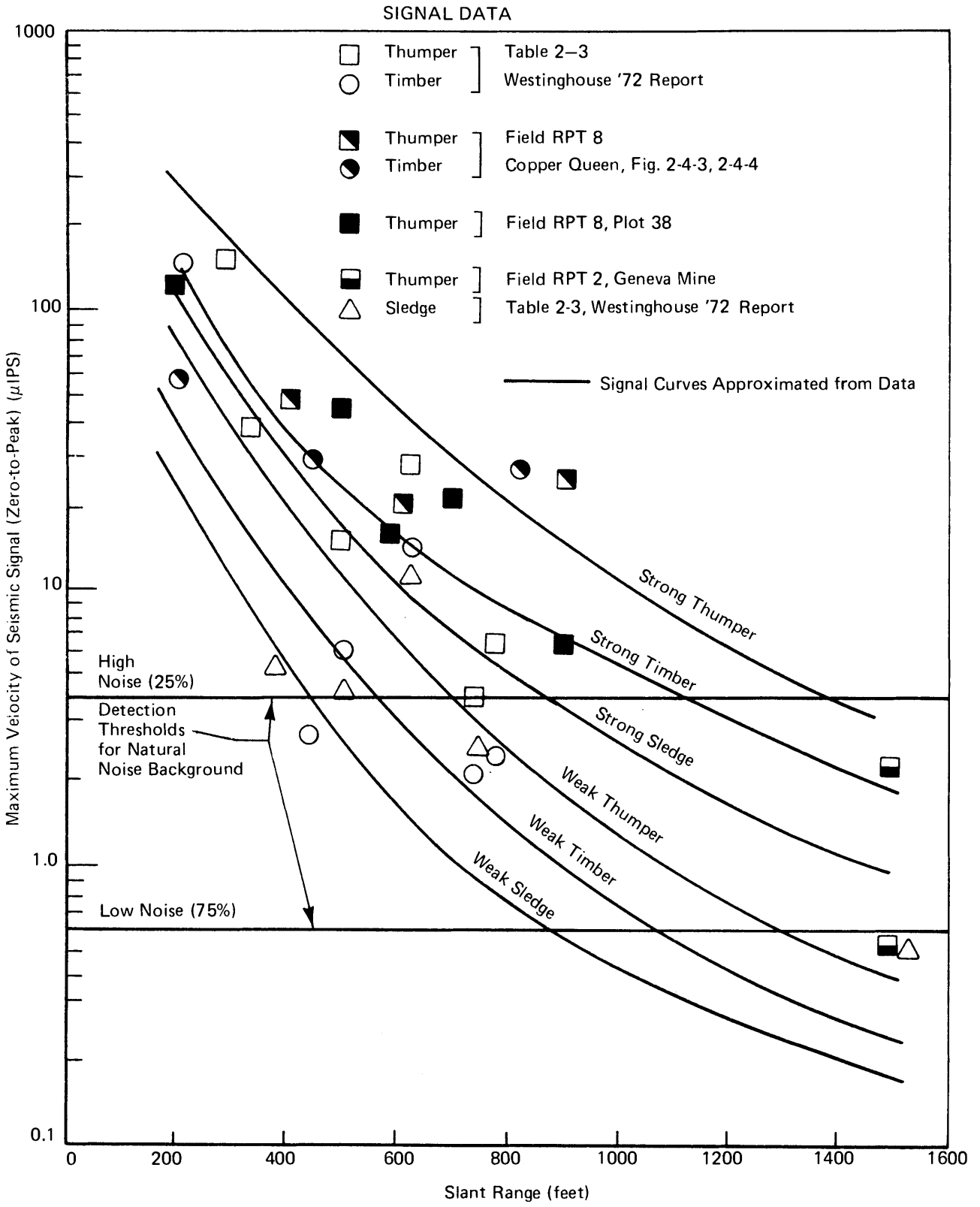

(Largest Zero to Peak Amplitude on Vertical Traces, Plotted for Three Sources, Thumper, Timber, Sledge Hammer.)

Signal Data from Westinghouse 1972 Report, Estimated Detection Thresholds also shown for **Natural Seismic Noise Background** (Noise Data from Frantti, 1963).

FIGURE 5 SEISMIC SIGNAL AMPLITUDE PLOTTED VERSUS SLANT RANGE FROM TYPICAL SOURCES

and weak signals for the thumper, timber, and sledge sources. These curves enclose the majority of the data, and are the basis of the detection range discussion in the next chapter. We believe that Figure 5 represents the best estimates of signal level that we can make at this time, based on experimental data available to us.

A scatter of a factor approximately 5 exists in the amplitude data. However this is not unexpected. Scatter of this magnitude is quite common in seismic data around 1 Hz, and can reflect any one of a number of factors. In the case of the Westinghouse data these factors probably include source coupling, propagation effects, the source radiation pattern, and variation of the low velocity alluvium thickness at the seismometer.

We have attempted to assess the source radiation pattern effect using the data from Field Report 8*, Copper Queen Mine, Figures 2.4.3 and 2.4.4, compiled in Table 2.4-3 of that report. In Table 3, we show their amplitude readings for both first motion and for maximum trace amplitude. Only the vertical seismometer is used. Also shown is the theoretical amplitude, V_m, of the vertical component for a point vertical source in an infinite medium. The V_m for such a source is of the form (Love, 1944, p. 304-305).

$$V_m = \frac{A}{r} \cos^2 \theta \qquad (2)$$

where r is slant range

θ is the angle between the vertical and the source-to-receiver direction

and A is a constant

The formula given is strictly valid only if the receiver is many wavelengths from the source. This requirement is not well met in the present experiment. We have set A to fit the observed amplitude at the seismometer on the surface directly above the source, receiver 1. The source and receiver locations are shown in Figure 6. Values for a 1/r variation are also given. Again we normalized to receiver 1.

The results in the Table are not conclusive. However in general, the 1/r fit is closer than the V_m fit. The V_m often greatly underestimates the amplitude.

The data, on Figure 5 obtained from plot 38 of Field Report 8*, (plot 38 is reproduced here as Figure 7a) is of interest. These data were obtained for a thumper source put in the Copper Queen Mine, 900 feet below the surface.

* Ibid.

Table 3

Source Pattern Effects (Copper Queen Mine)

a) First Motion Peak (μIPS)

	Receiver		
	1	2	3
Source (1), Timber			
Observed	54.	11.8	6.7
Theory, V_m	54.	5.3	0.58
1/r Variation	54.	24.	13.
Source (2), Thumper			
Observed	26.6	20.	8.6
Theory, V_m	26.6	8.	2.6
1/r Variation	26.6	17.	11.6

b) Maximum Trace Amplitude (μIPS)

	Receiver		
	1	2	3
Source (1), Timber			
Observed	58.3	29.8	27.1
Theory	58.3	5.6	0.67
1/r Variation	58.3	26.	14.2
Source (2) Thumper			
Observed	38.0	20.0	26.6
Theory	38.0	17.0	3.7
1/r Variation	38.0	34.0	17.

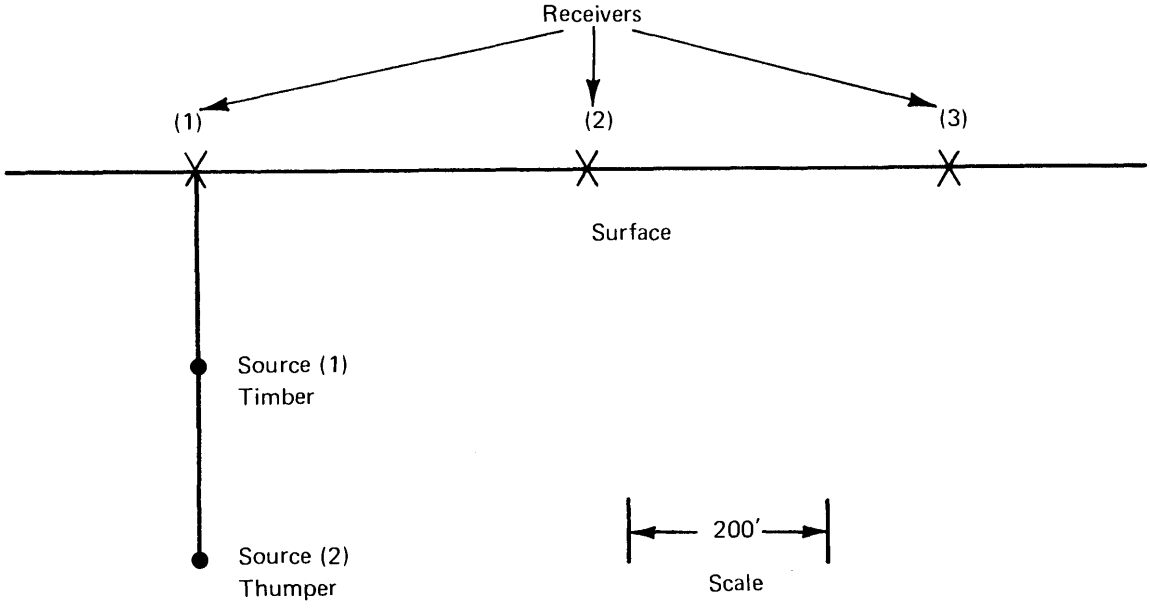

FIGURE 6 **SOURCE-RECEIVER LOCATIONS FOR COPPER QUEEN MINE WESTINGHOUSE SIGNAL STRENGTH EXPERIMENT**

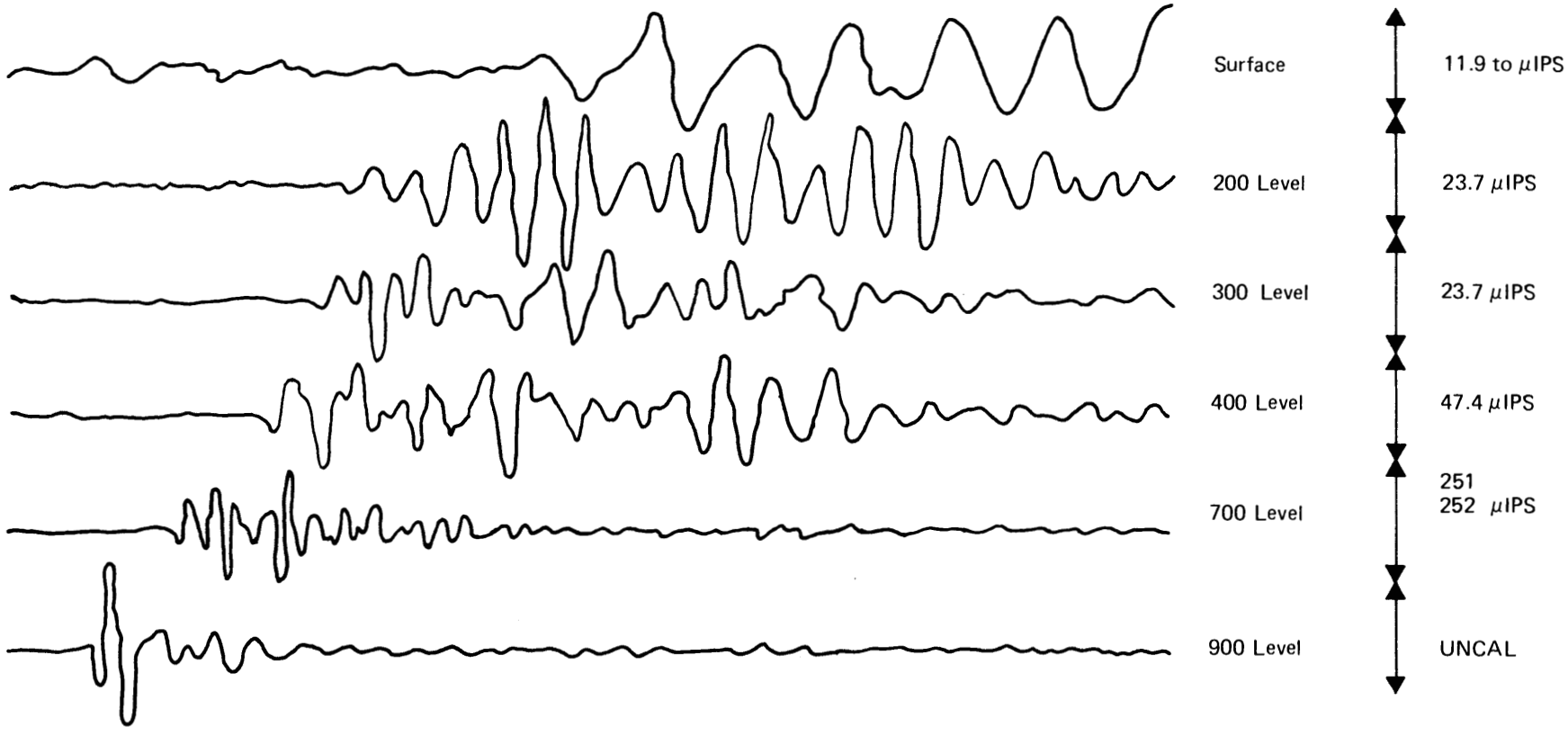

FIGURE 7(a) PLOT 38 FROM WESTINGHOUSE FIELD REPORT NO. 8
(Uplink Velocity and Attenuation – Thumper on 900 Level – 17 Blows)

Seismometers were at the 700', 400', 300', 200', and surface levels directly above the source. The fall-off of amplitude is slightly greater than 1/r. Another important observation is that the surface seismometer has a peak frequency of about 50 Hz while the peak frequency on the below-surface seismometer (at 200 feet) is about 100 to 125 Hz.

The amplitude on the surface seismometer is only about 1/3 that of the seismometer at the 200' level. The reason for the change in amplitude may be either attenuation in the low velocity surface layer or a resonance effect on the waves due to the low velocity surface layer. There is some indication that the latter is the major factor. Namely, plot 39 of Field Report 8* (reproduced as Figure 7b) reveals that an initial ∿100 Hz signal is propagated downward through the surface layer from a surface source to the below-surface seismometers. However, the initial part of the signals are followed in time by ∿40 Hz energy leaking downward from the resonant surface layer.

It is felt that further systematic experiment, and theoretical analysis of relevant models of source and propagation effects, are required to improve estimates of the signal strength and character in various mine situations.

V. DETECTION RANGES - BASED ON EXPERIMENTAL DATA

The initial discussion of detection range will be for a single sensor. It is based on Figure 5 which gives estimated signal levels and the detection thresholds required under two noise conditions. The detection level is set to give one false alarm every 100 seconds on a single subarray trace, so at this level it will be necessary to detect on perhaps three subarrays to safely conclude that a true signal has been received. Consistent relative arrival times on the subarrays will be a strong indication of a repeated source at a fixed location.

In Table 4 we give the maximum slant ranges for detection for different combinations of source and noise conditions. The values in the Table are the best estimates of detection range we can make at this time based on the experimental data available.

* Ibid

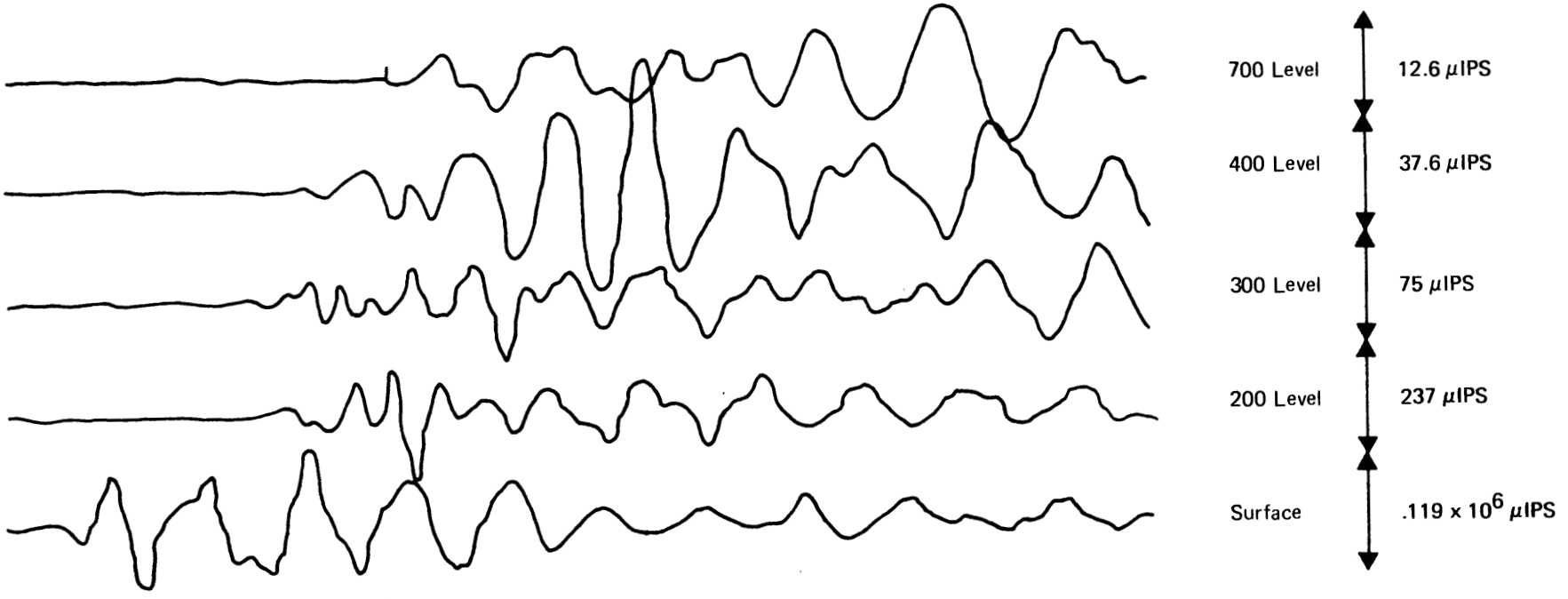

FIGURE 7(b) **PLOT 39 FROM WESTINGHOUSE FIELD REPORT NO. 8**
(Downlink Velocity and Attenuation – Timber on Surface – 10 Blows)

Table 4

Maximum Slant Range for Detection (Feet)
For a Single Sensor--Before Signal-to-Noise Improvement Techniques
(For Natural Noise Conditions)

Source	Natural Noise Condition: Low (75%) Threshold	Natural Noise Condition: High (25%) Threshold
Strong Thumper Signal	> 2000.	1400.
Weak Thumper Signal	1300.	700.
Strong Timber Signal	> 2000.	1050.
Weak Timber Signal	1100.	550.
Strong Sledge Signal	> 1500.	900
Weak Sledge Signal	900.	450.

At this point we make some speculative estimates of the detection thresholds required under conditions for which the noise data base is weak, namely for "maximum" natural noise conditions. By inspection of Figures 1, 2, and 3, it appears that the natural noise level rarely rises about 3 times the 25% detection threshold of Figure 5. This threshold,denoted as Max., is shown on Figure 8. Also shown are the signal level curves. We speculate that S/N improvement techniques can give a gain of 10 dB at all three noise levels. The figures of 10 dB would be the S/N gain against uncorrelated noise for a 10 element subarray. Gain obtained by burial could also be significant. In high levels of natural noise due to wind or rain the gain by burial could be considerably above 10 dB. Since there is presently no data to assess these gains we have taken the modest value of 10 dB between the two. On this basis we also put curves for the three noise level conditions with 10 dB S/N improvement on Figure 8. For these conditions, the estimated detection ranges are given in Table 5.

Further experimental data must be analyzed before we can make any estimate of the detection ranges in the presence of man-made noise of the type and level which might be present during uncontrolled rescue operations. However it is highly probable that heavy man-made noise would make detection impossible, using only surface seismometers, if the signaling miner is more than tens of feet to a few hundred feet from the seismometer.

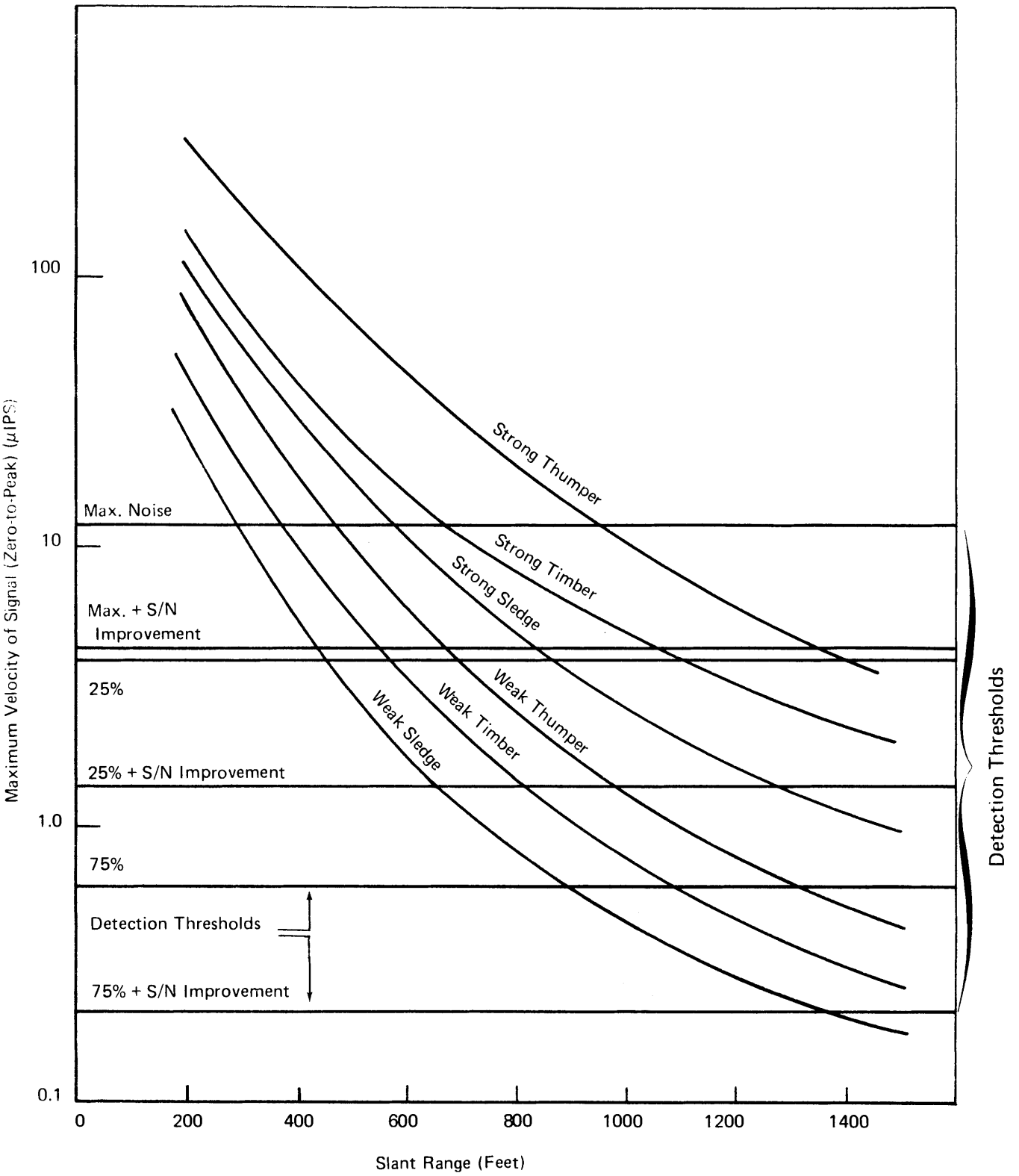

Seismic Signal Amplitude Estimates Plotted Versus Slant Range from Typical Sources; Detection Thresholds for Three Natural Noise Conditions With and Without Benefits of 10 dB Signal-to-Noise Improvement

FIGURE 8 COMPOSITE PLOT FOR ESTIMATING DETECTION RANGES

Table 5

Maximum Slant Range for Detection (Feet)

(For Natural Noise Conditions Only)

Source	Natural Noise Conditions			
	Max.	Max. +	25% +	75% +
Strong Thumper Signal	950	1400	>2000	>2000
Weak Thumper Signal	425	700	1000	>2000
Strong Timber Signal	650	1050	>1500	>2000
Weak Timber Signal	375	550	800	>1500
Strong Sledge Signal	550	900	1250	>2000
Weak Sledge Signal	300	450	625	>1400

(+) Indicates: +10 dB S/N Improvement

VI. EFFECT OF NOISE LEVELS ON ARRIVAL TIME ESTIMATION ACCURACY - BASED ON EXPERIMENTAL DATA

The two limits on the accuracy of the location of the miner are the accuracy of the velocity model and the accuracy of the reading of the arrival time of the P wave. The effects of deficiencies in the velocity models are discussed elsewhere. Here we concentrate on errors in arrival time measurement due to the presence of seismic background noise. Higher signal-to-noise ratios are needed for accurate estimates of arrival times than that needed to simply detect a miner-generated signal. Therefore, it is assumed that the signal-to-noise ratio is improved by stacking repeated signals, if signal repetitions have been received.

We discuss the errors in arrival time with reference to the schematic generalized signal shown as Figure 9. This signal illustrates several features of the signal waveforms which can affect the measurement of signal arrival time. Several examples of these features are shown in Figures 10a, b, and c, which are tracings of actual seismic signals taken from the Westinghouse Field Reports* (see Table 6 for identifications). The signal in Figure 9 has a frequency of 50 Hz (period, T = 20 ms) which is an average frequency for the signals observed by Westinghouse.

* Ibid

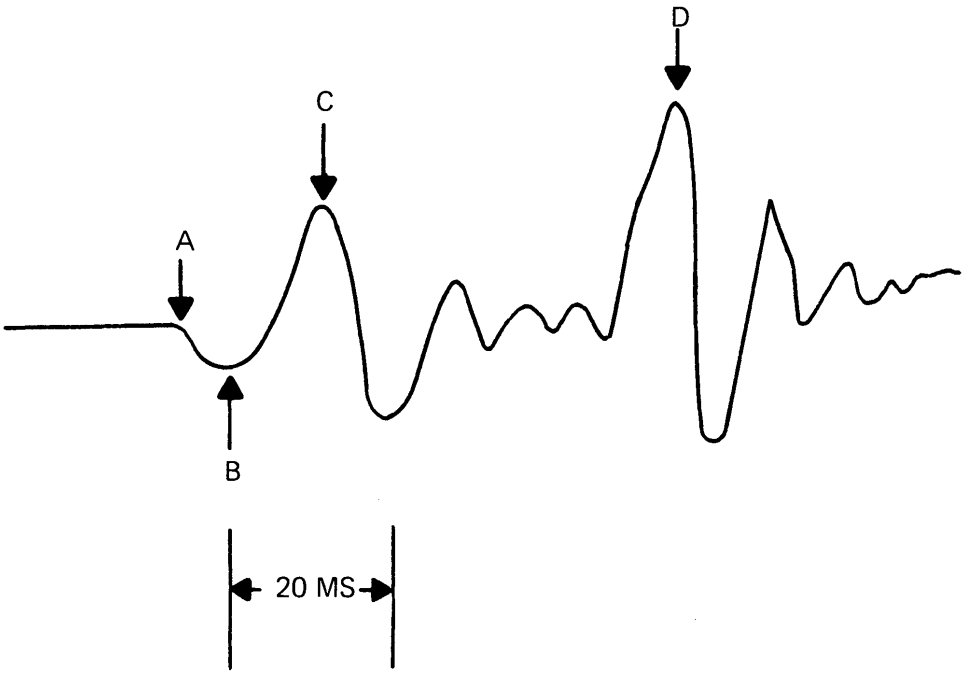

FIGURE 9 SCHEMATIC GENERALIZED SEISMIC SIGNAL
(Applicable to Mine Data Obtained to Date)

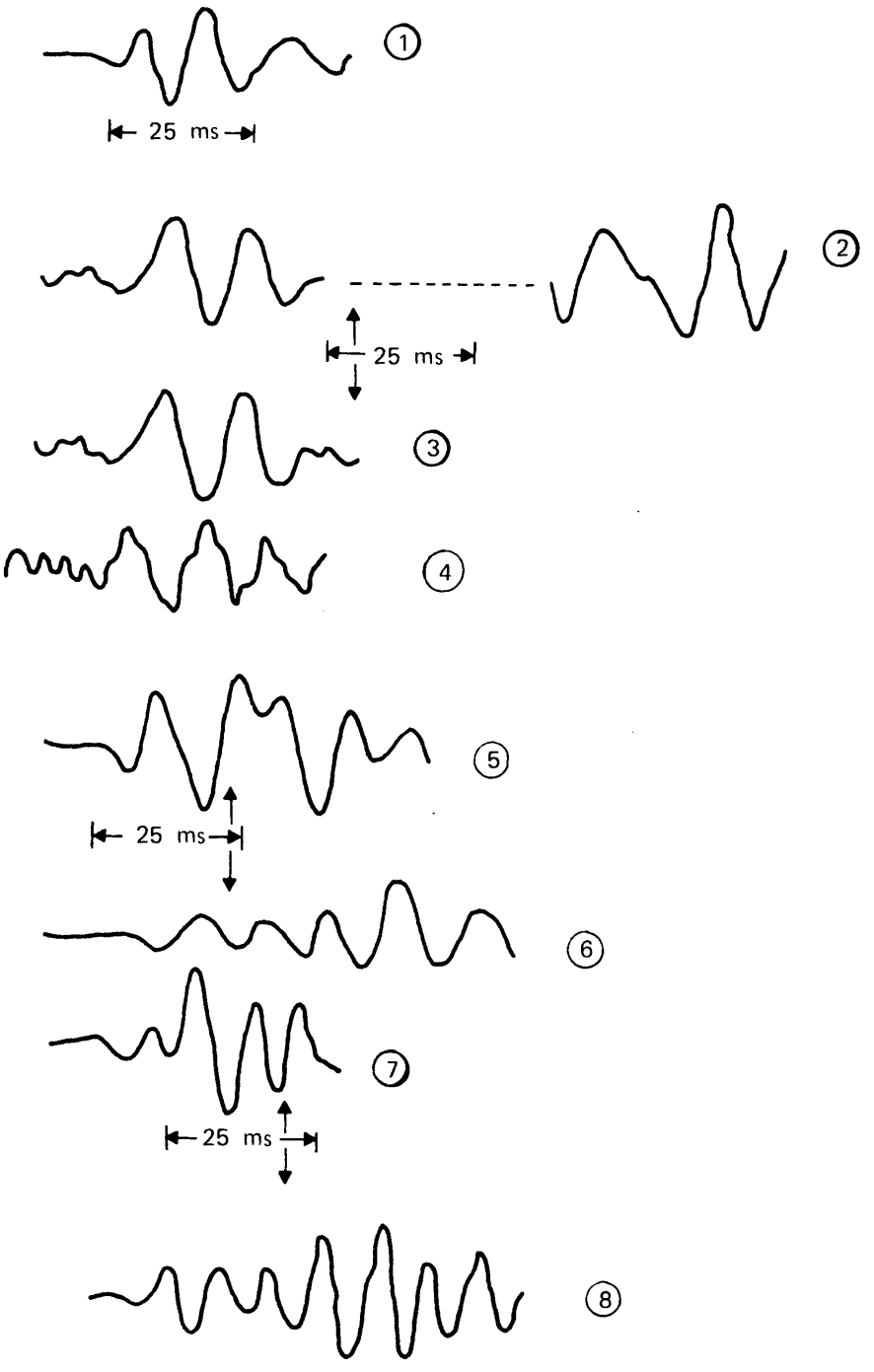

FIGURE 10(a) TRACINGS OF ACTUAL SUMMED SIGNALS FROM WESTINGHOUSE FIELD REPORTS

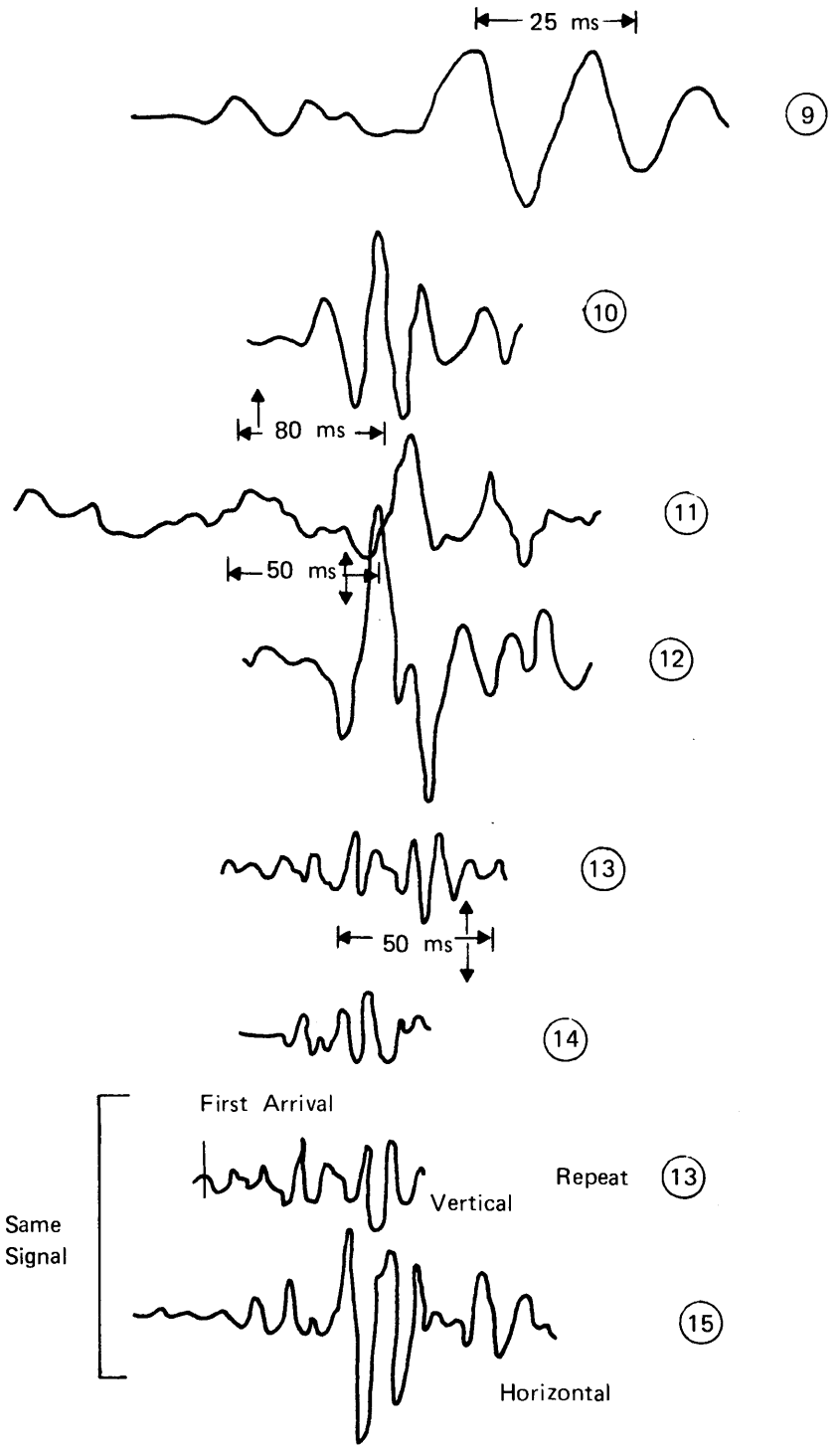

FIGURE 10(b) TRACINGS OF ACTUAL SUMMED SIGNALS FROM WESTINGHOUSE FIELD REPORTS

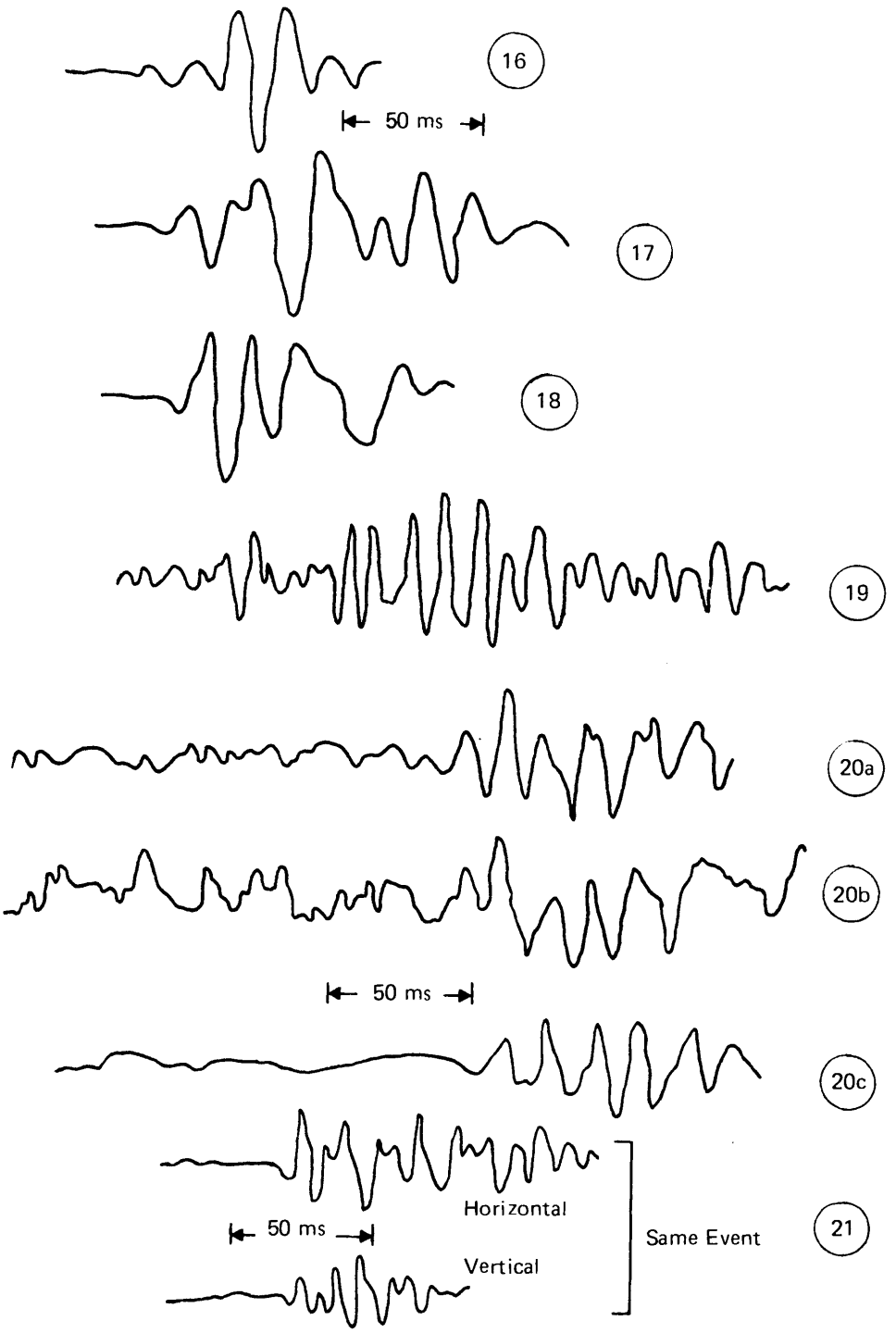

FIGURE 10(c) TRACINGS OF ACTUAL SUMMED SIGNALS FROM WESTINGHOUSE FIELD REPORTS

Table 6

Legend for Tracings of Actual
Summed Signals Shown in Figures 10a, b, & c

Tracing No.			
1.	Plot 23 F.R. 6	- 13 element subarray, 30 blows	Figure 10(a)
2.	Plot 35 F.R. 4	- 7 elements , 50 blows	
3.	" "	- 1 vertical , " blows	
4.	37	- 1 vertical , 30 blows	
5.	Plot 37 F.R. 7	- Array (subarray?) 2, 30 blows	
6.	Plot 41 "	- Array 7, 30 blows	
7.	Plot 42 "	- Not known 30 blows	
8.	Plot 39 "	- Array 5 " blows	
9.	Plot 36 "	? " blows	Figure 10(b)
10.	Figure 17, F.R. 2, ch. 5, South		100 blows
11.	Figure 22, F.R. 2, ch3, 19 Hex array		31 blows
12.	Figure 24, F.R. 2, 7 elements		100 blows
13.	Plot 15, F.R. 8, ch 5		15 blows
14.	" "	ch 2 " blows	
15	" "	ch 7, Horizontal "	
16.	Plot 17 "	ch 7, 30 blows	Figure 10(c)
17.	" "	ch 4, "	
18.	Plot 55 "	ch 6, 25 blows	
19.	Plot 57 "	ch 3, Array K, 700' level, 29 blows	
20.	Plot 36 "	comparison of small arrays and single geophone, a) single channel, b) parallel, c) series correction	
21.	Plot 15, F.R. 8, ch 2 and 3, horizontal and vertical, 15 blows		

We assume that the arrival time is picked by a trained analyst, and we discuss the arrival time errors which might arise for different levels of noise. The true arrival time of the signal is T_A. [T_A is the time of the signal at point A and the other times used (T_B, T_C, T_D) are similarly defined.] If the noise level is very low, the analyst will pick the arrival time, denoted by AT, within 1 ms of T_A. The first peak B of the signal is usually small compared to the second peak C. If the noise level is only low enough to recognize peak B, then he picks T_B as the arrival time. This gives an error of about 4 ms. However, it would be better to assume that $T_B = T_A + T/4$. If this is done the error in AT will probably be reduced to on the order of 2 ms.

A much larger error in arrival time can occur in cases when peak D is larger than peak C, and the noise level is such that the analyst misses peak C, but can pick peak D. Examples of signals where peak D is larger than peak C are shown in Figure 10 as traces 6, 8, and 13. Peak D may be 6 dB above peak C. By picking T_D, several cycles of the signal have been missed and the error in arrival time will be 50 to 100 ms. If T_C is picked on some subarrays and T_D on others, very poor locations will result.

There are fortunately some telltale indications if the initial few cycles of the signal have escaped detection, and T_D was picked as the arrival time by mistake. First if T_D is picked on only one or two of seven subarrays, these times will show up as large, late residuals on the least squares fit for the source location. A second indication is that a very large signal may occur on the horizontal seismometers at T_D. An example of this large horizontal motion is shown on Figure 10, traces 13 and 15 and 21. We believe the large late arrivals may be the direct S (shear wave), or a shear wave generated when the P wave hits the base of the alluvium layer below the receiver. A better understanding than we presently have might allow a better possiblity of telling whether the first arrival picked by the analyst is a T_D type late arrival.

VII. EFFECT OF ALLUVIUM ON ARRIVAL TIME ESTIMATION ACCURACY

The surface alluvium has a very low P wave velocity. The velocity can be 2000 feet/sec. or even less. Suppose at a mine we have 50 feet of alluvium under subarray A and no alluvium under subarray B. Let the rock P wave velocity be 10,000 feet/sec. Then the traverse time through the alluvium at

subarray B will be 5 ms. Thus if a location is made with these arrival times with no correction for the presence of the alluvium at A, the 20 ms extra delay at A will have the effect of a 20 ms arrival time reading error.

A example of this delay can be observed directly in Figure 11. In Field Report 8*, data is given for a source at 900 feet depth with receivers at various depths and on the surface. In our figure the arrival times are plotted versus distance from the source. If the travel time curve is extrapolated from the straight line fit to the last 3 underground arrivals, the time predicted for the surface arrival is 16 ms earlier than the observed arrival time at the surface.

This problem of the error in arrival time due to the alluvium can be corrected by determining the thickness and velocity of the alluvium at each subarray. This can probably best be done by an easily run shallow refraction survey using either a timber or perhaps a seismic thumper as a source. Reflection seismic methods, using special equipment, might also be useful. Another method which might prove useful,which we have used at Penn State,is to use the dispersion properties of the Rayleigh waves set up with a sledge source.

VIII. RECOMMENDED PROJECTS

In order to improve the performance estimates presented in this Part; to better evaluate the utility of signal-to-noise improvement techniques such as seismometer burial, bandpass filtering, subarrays, and signal stacking; and to develop more effective signaling and detection strategies; the following experimental and theoretical efforts are recommended.

● Perform a series of careful seismic noise and signal strength measurements in Eastern coal mining regions. These measurements should be performed by crews well-experienced in seismic and geophysical field work. At each of the sites care should be taken to determine the geological/seismic structure of the overburden material, so that the experimental results can be compared with those predicted by different theoretical models.

- Seismic noise measurements should be performed in representative Eastern mining areas that are "quiet", i.e. not dominated by manmade noise sources; and in areas and under circumstances that are representative of those encountered during mine emergencies or disasters. Noise spectrum levels should be obtained up to a frequency of 300 Hz. The spatial coherence properties of the noise should be studied as a function of seismometer spacing,[4,5] together with the utility of looking at individual seismometer outputs as opposed to that from a whole subarray. The impact of the depth and method of seismometer

* Ibid

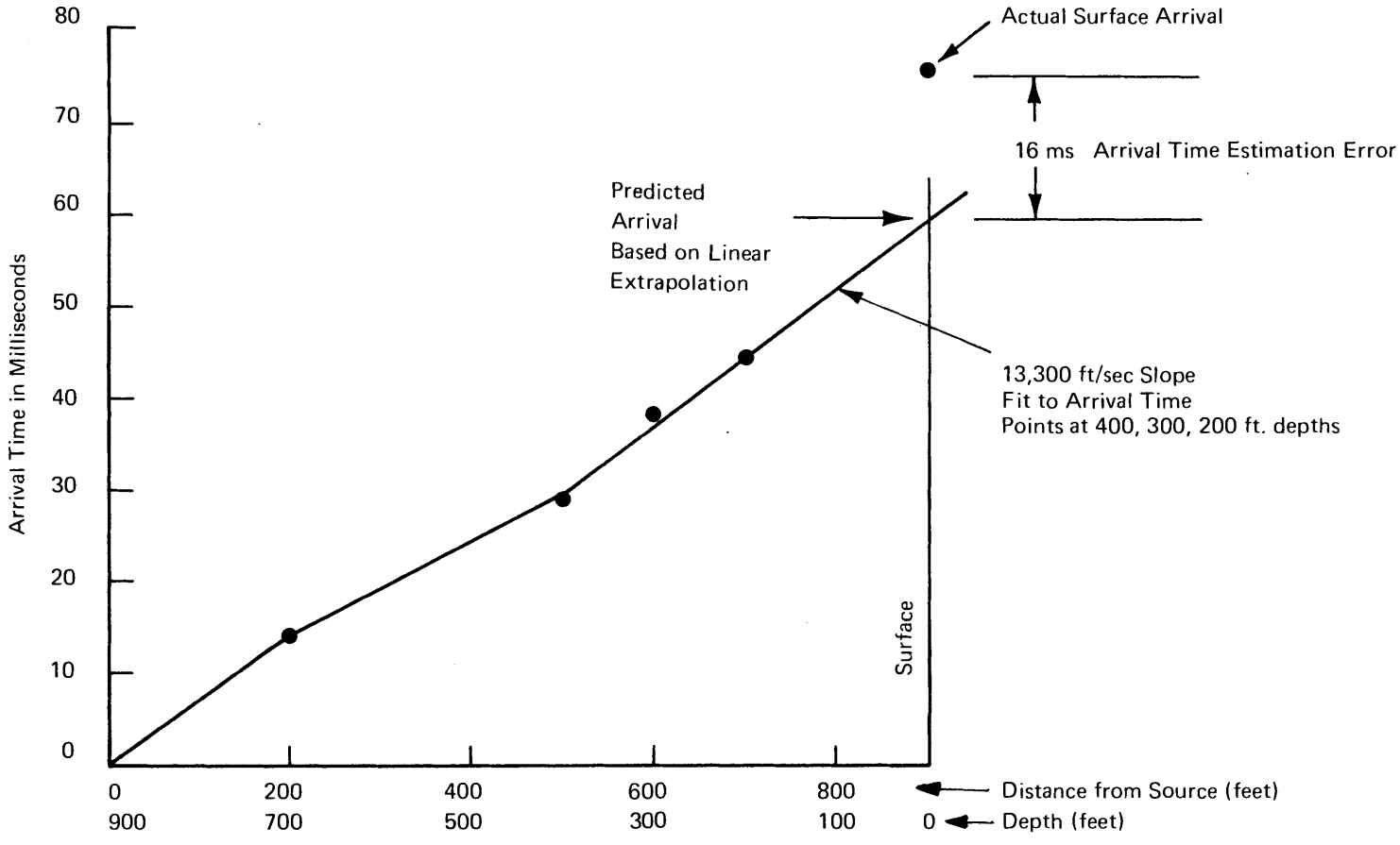

Data from Field Report 8, Plot 38.

FIGURE 11 EXAMPLE OF TIME DELAY CAUSED BY SURFACE WEATHERED ALLUVIUM LAYER

burial on the received seismic noise should be examined by careful experiments at sites with different surface materials. At sites over mines where both signal and noise measurements are planned, the effect of seismometer burial on both received signal and noise levels should be determined. Lastly, representative manmade sources encountered during mine emergencies should be characterized, together with some of the likely disaster noise sources in the mine, such as fires, running water, cracking rocks, and roof falls.

- Controlled, systematic seismic signal experiments should be performed with the thumper, timber, sledge, and perhaps other practical sources, in several Eastern coal mines that are representative with respect to depth, overburden geology, and surface topography. Signal properties, such as strength and frequency content, of single source blows or pulses should be examined as a function of type of source, entry cross-sectional dimensions, position and composition of the impact area in the entry, source and seismometer depths, slant range, near-surface layers, and seismic velocity profile. The measurement band should extend up to a frequency of about 300 Hz, to check whether useful signal frequency content above 100 Hz may have been masked by system noise or lossy surface layers in past measurements.

● Perform supporting theoretical analyses to better understand the signal generation and propagation behavior expected for practical miner sources in coal mines. Items of particular interest are: the efficiency of seismic signal excitation, the effect of the mine entry cavity and the source impact point in it, the effects of layering in general and the surface layer in particular. Preliminary analysis indicates that it should be possible to model the mine entry problem as a point source applied to the surface of a cylindrical cavity; and that surface layering effects can be examined using Haskell[6] matrix techniques.

● Develop automatic detection procedures that will choose only the most "interesting" seismic energy arrivals, or probable miner signals, for detailed examination by a trained analyst. An automatic detection or event screening procedure need not be complex, and in its simplest form could be based on the exceedance of a preset threshold on one or more seismometers or subarrays, and set according to the prevailing noise condition. This should ease the large data processing burden that otherwise would be imposed on analysts under emergency conditions. However, it is not intended to replace the trained analyst, for he is the one who will be best qualified to assess the likely cause of the received waveform, and to subsequently ascertain its

"arrival time", after any required signal-to-noise ratio enhancement.

● Develop an ability to determine, in a timely manner on site, the thickness and seismic P-wave velocity of the alluvium directly under each of the subarrays. This is needed in order to compensate the signal arrival times for the likely substantial and different amounts of time the signal has spent in this low-velocity, variable-thickness, surface layer to get to each subarray.

IX. REFERENCES

1. Love, A.E.H., Mathematical Theory of Elasticity, Dover, New York, 1944.
2. Frantti, G.E., The Nature of High Frequency Noise Spectra, Geophysics, 28, 547-562, 1963.
3. Horton, C.W., Sr., Signal Processing of Underwater Acoustic Waves, U.S. Government Printing Office, Washington, D.C., 1969.
4. Capon, J., Greenfield, R.J., Lacoss, R.T., Design of Seismic Arrays for Efficient On-Line Beamforming", Lincoln Laboratory Technical Note, 1967-26, 27 June 1967.
5. Lacoss, R.T., Capon, J., Greenfield, R.J., "Preliminary Design of a Long Period Seismic Array for Norway", Lincoln Laboratory Technical Note, 1968-4, 24 January 1968.
6. Haskell, N. A., Crustal Reflection of Plane P and SV Waves, Journal of Geophysical Research, Vol. 67, No. 12, pp. 4275, pp. 4751-4759, Nov. 1962.

APPENDIX A

RELATION OF PEAKS OF NOISE ENVELOPE TO RMS LEVELS

The envelope of narrowband noise is given by the Rayleigh distribution (e.g. Horton, 1969, p. 96). The results we give below have experimentally been found to fit wideband seismic data, (see Capon et al. 1969). The probability density function is given by:

$$P(R) = \frac{R}{\sigma^2} \exp\left(-R^2/2\sigma^2\right) \qquad \text{(A 1)}$$

where R is the zero to peak amplitude of the envelope.

Over one cycle, the mean square (MS) value is

$$\frac{1}{T} \int_o^T y^2(t)\, dt = \frac{1}{2} R^2 \qquad \text{(A 2)}$$

Thus the MS value of narrowband noise is

$$\begin{aligned} MS &= E\left[y^2(t)\right] = \frac{1}{2} E\left(R^2\right) \\ &= \frac{1}{2} \int_o^\infty P(R)\, R^2\, dR \\ &= 2\sigma^2 \qquad \text{(A 3)} \end{aligned}$$

$$\text{or RMS} = \sqrt{2}\,\sigma \qquad \text{(A 4)}$$

The probability of R exceeding R_o is

$$P[R > R_o] = e^{-R_o^2/2\sigma^2} \qquad \text{(A 5)}$$

If we take R_o = 3 RMS

$$P\left[R > (3RMS)\right] = e^{-9} = .000123 \qquad \text{(A 6)}$$

Then the chances of the envelope exceeding 3 RMS on a single trial is about one in .000123. We take 3RMS as a reasonable single channel detection threshold. We note that for a bandwidth of 75 Hz we get an independent sample of R every 1/75 sec. Therefore we go about 100 seconds between false alarms on each channel.

A useful relationship in evaluating Frantti's (1963) method of spectral estimation is that

$$E\,[2R]/E\,[RMS] = 2\int_0^\infty R\,P(R)\,dR/E\,[RMS]$$

$$= \sqrt{\pi} = 1.77 \qquad \text{(A 7)}$$